Mem. S.A.It. Suppl. Vol. 8, 124
© SAIt 2005

Memorie della
Supplementi

Determination of $v \sin i$ with Fourier transform techniques

F. Royer

GEPI/CNRS UMR 8111, Observatoire de Paris, 5 place Janssen, 92195 Meudon cedex, France

Received / Accepted

Abstract. In this paper, the use of Fourier transforms to derive stellar projected rotational velocity — $v \sin i$ — is described. The main advantages of the representation in the Fourier domain come from the frequency behavior of the rotational profile, easier to visualize and to work with than in the wavelength domain. Some examples are taken from the literature.

Key words. technique: spectroscopic – stars: rotation

1. Introduction

Rotation is one of the fundamental stellar parameters and the many aspects of its importance in stellar formation and evolution can be found in the dedicated IAU Symposium (Maeder & Eenens 2004).

There are four basic methods for measuring axial stellar rotation, depending on the observed effect of rotation and on the type of object. To derive the signatures of axial rotation, one can analyze:

1. the spectral line profile broadening, which leads to the projected rotational velocity: $v \sin i$,
2. the photometric modulation of star light, in the case of stars with spots on their surface, which allows the derivation of the rotational period,
3. the Rossiter effect which distorts the radial velocity curve in some eclipsing binary systems,
4. the shape of the stellar disk, using interferometric measurement, to derive the oblateness of the star caused by rotation.

The first three methods are overviewed by Slettebak (1985), and the last and most recent one is detailed by van Belle et al. (2001). Methods 2, 3 and 4 are limited to specific objects: stars with spots (2), eclipsing binary systems (3), nearby and bright stars (4), whereas the first method can be applied to a very wide range of objects.

This paper will focus on (1), and the methods for measuring the $v \sin i$ parameter. Sect. 2 will detail the line profile broadening, Sect. 3 will overview the different methods for measuring the $v \sin i$. In Sect. 4, the Fourier transform technique is presented. In Sect. 5, different applications of the method to study rotation are shown.

2. Line broadening

The observed spectrum of a star, $s(\lambda)$, can be written as a double convolution (Gray 1992):

$$s(\lambda) = h(\lambda) * b(\lambda) * p(\lambda) \quad (1)$$

where $h(\lambda)$ is the "true" spectrum of the star, $b(\lambda)$ the broadening function, and $p(\lambda)$ the instrumental profile.

2.1. Rotational profile

Considering pure axial rotation of a homogeneous spherical rigid body, the rotational broadening is a semi-elliptic profile (Carroll 1928; Shajn & Struve 1929).

When adopting a linear law for the limb darkening [1], an additional parabolic term appears in the rotational profile:

$$b(\lambda') = \underbrace{c_1 \sqrt{1-\lambda'^2}}_{\text{elliptic term}} + \underbrace{c_2 (1-\lambda'^2)}_{\text{parabolic term}} , \quad (2)$$

with

$$\Delta\lambda = \lambda_0 \, v \sin i / c, \quad (3)$$

$$\lambda' = (\lambda - \lambda_0)/\Delta\lambda, \quad (4)$$

$$c_1 = \frac{2\,(1-\epsilon)}{\pi\,\Delta\lambda\,(1-\epsilon/3)}, \quad (5)$$

$$c_2 = \frac{\epsilon}{2\,\Delta\lambda\,(1-\epsilon/3)}. \quad (6)$$

In Fig. 1 one can see the effect of the limb darkening parameter ϵ on shape of the rotational profile. The effect of limb darkening is to reduce the contribution to the integrated spectrum from the regions near the limb.

2.2. Other sources of broadening

The broadening $b(\lambda)$ can be the convolution of different broadening mechanisms in Eq. 1. These mechanisms may have different profiles. The main mechanisms are briefly described below.

[1] Let θ be the angle between the surface normal and the line of sight to the observer. The local intensity will be a function of θ. Using a linear approximation, the intensity of light coming from the surface of the star is: $I(\theta) = I_0\,(1 - \epsilon(1 - \cos\theta))$, where ϵ is called the limb darkening coefficient.

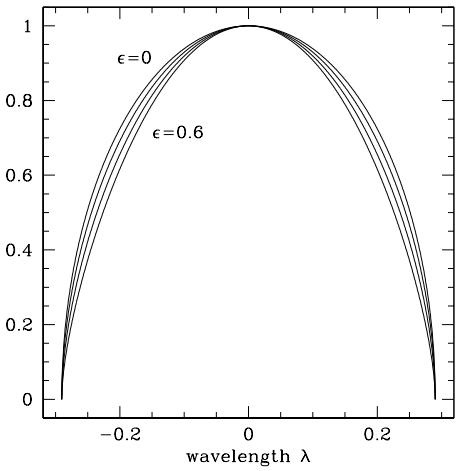

Fig. 1. Shape of a pure rotation broadening profile for different values of the limb darkening parameter: $\epsilon = 0$ (outer curve), 0.2, 0.4 and 0.6 (inner curve).

2.2.1. Pressure broadening

It results from collisions between molecules in a gas. Because an electron may radiate over a finite amount of time, the line shape can be well described by a Lorentzian profile:

$$b_{\rm L}(\lambda') = \frac{\alpha_{\rm L}}{\pi}\left(\lambda'^2 + \alpha_{\rm L}^2\right)^{-1}, \quad (7)$$

where $\alpha_{\rm L}$ is the Lorentzian half-width.

2.2.2. Turbulence

Different motions in the photospheric gas induce a broadening effect on the observed spectra. Depending on the size of the turbulent cells, these effects are called micro- or macroturbulence, and they are represented with Gaussian profiles.

2.2.3. Instrumental effects

The instrument profile $p(\lambda)$ is another source of broadening. This point-spread-function is usually assumed to be Gaussian, but as it is instrument dependent, can be accurately computed using external calibration data. The resolving power, estimator of the width of the

instrumental profile, is a limitation to the determination of the $v \sin i$. The empirical rule of thumb says that the lower limit in $v \sin i$ in $\mathrm{km\,s^{-1}}$ is equal to the dispersion in $\mathrm{\AA\,mm^{-1}}$.

3. Measurement of the $v \sin i$

Many measurements of $v \sin i$ can be found in the literature (Głębocki & Stawikowski 2000), and the major part of them are derived from the broadening in wavelength space. Even if the entire line profile can be fitted, it is easier and quicker to measure $v \sin i$ on the basis of one single parameter: the full width at half maximum (FWHM). Slettebak et al. (1975 and earlier papers) give calibrations of $v \sin i$ against FWHM.

Another approach can be applied for low velocity rotators to take benefit of a wide wavelength range: the width of the cross-correlation function of the spectrum with a template can be used to derive the rotational broadening. Melo et al. (2001) apply this technique to FEROS spectra of low velocity rotators in M67.

Carroll (1933) first used the Fourier transforms to measure $v \sin i$ in the frequency domain, and the following sections emphasize these techniques.

4. Fourier transform approach

Many details and explanations about the analysis using Fourier transforms can be found in Smith & Gray (1976) and Gray (1992). The following sections will give some highlights.

4.1. Line profile in Fourier domain

The convolution theorem tells us that Eq. 1 is equivalent to

$$S(\nu) = H(\nu)\, B(\nu)\, P(\nu), \tag{8}$$

where S, H, B and P are respectively the Fourier transforms (hereafter FT) of s, h, b and p.

1. If the intrinsic profile of the line $h(\lambda)$ is close enough to a Dirac impulse function, then in the frequency domain, $H(\nu)$ is a constant function and thus negligible.
2. The Fourier transform of a semi-elliptic profile is dominated by a Bessel function of the first kind[2] (Fig. 2). Moreover the additive contribution of the parabolic term in frequency shows similar oscillations[3]. The function $B(\nu)$ thus oscillates, with an amplitude envelope decreasing with increasing frequency.
3. Assuming a Gaussian instrumental profile $p(\lambda)$, $P(\nu)$ is also a Gaussian function (Fig. 2).

4.2. Measuring rotation

The first use of FT to derive rotational velocity were done in the 1930s. Carroll (1933) shows that the $v \sin i$ parameter can be derived from the zero loci of $B(\nu)$: ν_1, ν_2, ν_3 ...

These zero loci are inversely proportional to the $v \sin i$, so that in a logarithmic frequency scale, a change of the rotational profile velocity toward higher (respectively lower) $v \sin i$ corresponds to a shift of the profile to lower (respectively higher) frequency. It is then easy to shift a theoretical profile for a given $v \sin i$ to match any observed rotational profile and then both derive the $v \sin i$ and check the shape of the observed profile. Figure 3 shows an example of theoretical and observed rotational profiles.

[2] The Fourier transform of a function f_1 defined by

$$f_1(\lambda) = \begin{cases} \sqrt{1-(\lambda/\Lambda)^2}, & \text{if } |\lambda| < \Lambda, \\ 0, & \text{if } |\lambda| > \Lambda, \end{cases}$$

is

$$F_1(\nu) = \frac{\sqrt{2\,\pi}\, J_1(\Lambda\,\nu)}{2\,\nu},$$

where J_1 is the Bessel function of the first kind of order 1.

[3] The Fourier transform of a function f_2 defined by

$$f_2(\lambda) = \begin{cases} 1-(\lambda/\Lambda)^2, & \text{if } |\lambda| < \Lambda, \\ 0, & \text{if } |\lambda| > \Lambda, \end{cases}$$

is

$$F_2(\nu) = \frac{2}{\Lambda^2}\sqrt{\frac{2}{\pi}}\left(\frac{\sin(\Lambda\,\nu) - \Lambda\,\nu\,\cos(\Lambda\,\nu)}{\nu^3}\right).$$

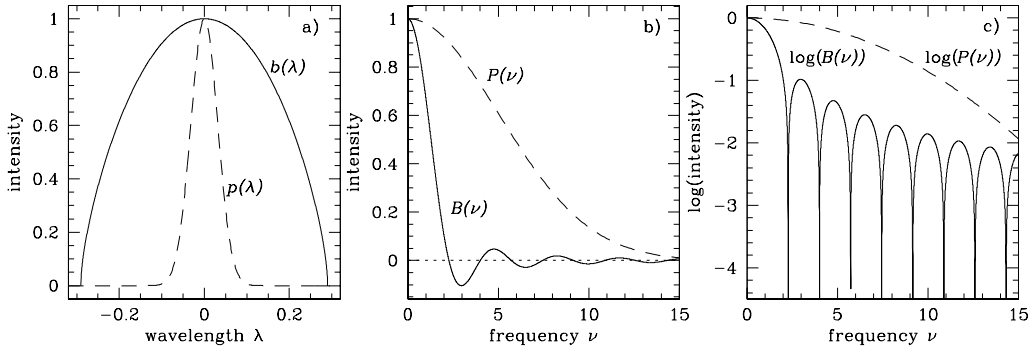

Fig. 2. a) Example of rotation profile $b(\lambda)$ (with $\epsilon = 0.6$) and Gaussian instrumental profile $p(\lambda)$. In this case, the rotational broadening is about 6 times larger than the FWHM of the instrumental profile. **b)** Fourier transforms of $b(\lambda)$ and $p(\lambda)$: $B(\nu)$ and $P(\nu)$ respectively. The dotted line is the zero x-axis which intersects $B(\nu)$ in ν_1, ν_2, ν_3 ... **c)** Same as b) with a logarithmic scale in y-axis, taking the logarithm of the absolute values of $B(\nu)$ and $P(\nu)$.

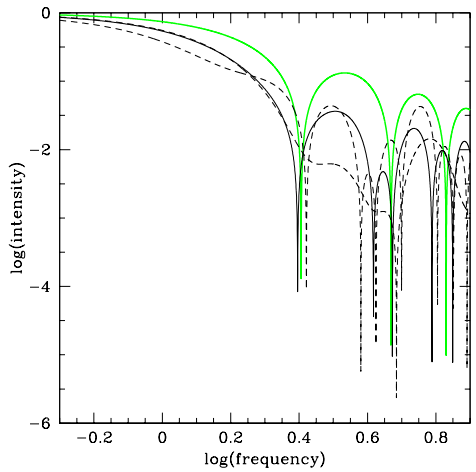

Fig. 3. Example of comparison between observed (back) and theoretical (green) rotational profiles. The three observed profiles correspond to three different spectral lines of a given spectrum, and the two dashed-line profile are discarded due to the shape of their first lobe (compared to the theoretical profile), whereas the solid-line one is used to derive the $v \sin i$ value.

The loci ν_k vary with limb darkening and Dravins et al. (1990) give the polynomial fit of the position variations of the first three zeros of the rotational profile with ϵ.

Similarly to the determination in the wavelength domain, $v \sin i$ in frequency domain can be derived from one single parameter: the first zero of $B(\nu)$. The relative zero loci provide informations about non-spherical rigid body rotation. Reiners (2003) details the variations of ν_2/ν_1 due to solar-like differential rotation, and gravity darkening.

The amplitude of the sidelobes of $B(\nu)$ decreases with increasing ν, and it is amplified by the instrumental profile. Thus the quality of the data sets limitation on the furthest measurable zero locus on $B(\nu)$.

5. Applications of Fourier techniques

5.1. Single line profiles

The rotational profile $b(\lambda)$ can be approximated by observed line profiles $h(\lambda)$. These candidate spectral lines shall be:

- not blended, so that the intrinsic profile in Fourier space does not add zeros in the frequency range used for $v \sin i$ derivation,
- close to continuum, for reliable normalization,
- intense enough to be measurable when rotation increases,
- dominated by rotation (e.g., no Balmer line ...).

Under these conditions, the FT of the line profile can be analyzed to derive the zero loci.

Contamination by the intrinsic profile: Even if the lines are chosen carefully, the observed profile encompasses larger wavelength range with increasing $v \sin i$, and blends affect the observed profile. This contamination can add zeros to the FT and give spurious results in $v \sin i$ determination. Such effects are illustrated by Mora et al. (2001) who compare the FT of observed profiles with corresponding synthetic zero-rotation FT profiles.

Contamination by the instrumental profile: The instrumental resolution also affects the observed profile. It does not add zeros to the Fourier profile but lowers the amplitude of the sidelobes with increasing ν, and imposes, together with the noise level, an upper-limit to the frequencies where $v \sin i$ can be derived.

Royer et al. (2002a,b) use this method on different data samples of A-type stars. They derive $v \sin i$ values for candidate spectral lines in the range 4200–4600 Å, and use a priori (based on the spectral type) and a posteriori (based on the FT shape) selections to reject unreliable lines. The mean $v \sin i$ value is kept as the stellar projected rotational velocity and the associated standard deviation is used to estimate the error. This precision is found to be ~ 5 % of the $v \sin i$ value.

5.2. Broadening function

The aim of choosing single lines for deriving $v \sin i$ is to avoid contamination by the intrinsic profile. Another method is to get rid of the intrinsic profile, and study directly $B(\nu)$. Reiners & Schmitt (2003) use a "Physical Least Squares Deconvolution" to extract an overall broadening profile using a large wavelength range. Starting from a δ-template, they adjust the equivalent width of each line and finally deconvolve the overall broadening profile $b(\lambda)$. Then, the analysis of the broadening profile is done in the Fourier space, on $B(\nu)$.

This technique allows the investigation of higher Fourier frequencies by both increasing the signal-to-noise in the Fourier domain, and removing possible zeros from the intrinsic profile. The obtained accuracy allows the detection of signature of gravity darkening or differential rotation (Reiners 2003). Reiners & Royer (2004b) apply this method to sample of 74 A-type stars, and detect four possible differential rotators among the studied stars. Reiners & Royer (2004a) apply this method to a high signal-to-noise ratio spectrum of Altair, and the effect of gravity darkening allows them to estimate the inclination angle i of the rotational axis using spectroscopic analysis.

6. Conclusions

To summarize, the main advantages of the Fourier analysis for $v \sin i$ determination are:

- it is calibration independent, contrary to the use of the FWHM; the theoretical first (and second) zero locus for the given ϵ is the only needed input,
- it allows an easy diagnostic of the rotational origin of broadening, by comparing to a theoretical profile,and therefore one can safely remove non reliable lines. It also allows the identification of differences to spherical rigid body rotation, such as differential rotation or gravity darkening whose signatures can be detected on the rotational profile in Fourier space.

Table 1. Examples of spectral lines used to derive the $v \sin i$ with Fourier transform analysis in the literature, for different ranges of spectral types.

Spectral types	Lines used for $v \sin i$ determination
early-mid B	He I 4388 Å, He I 4471 Å, Si III 4568 Å, ...
late B, A	Fe I 4405 Å, Mg II 4481 Å, Ti II 4501 Å, ...
F, G type	Fe I 4989 Å, Fe I 6265 Å, Ca I 6439 Å, ...
K type	Fe I lines $\sim$ 6250 Å, ...

In the literature, the Fourier method is applied to many spectral types. Some examples of spectral lines used to derive $v \sin i$ with Fourier method are given in Table 1. When single line profiles are used, this method can be applied also to binary objects showing composite spectra, provided that the component lines are not blended. Using a global broadening function provides very accurate results even for fast rotators whose spectra are heavily blended.

References

Carroll, J. A. 1928, MNRAS, 88, 548

Carroll, J. A. 1933, MNRAS, 93, 478

Dravins, D., Lindegren, L., & Torkelsson, U. 1990, A&A, 237, 137

Głębocki, R. & Stawikowski, A. 2000, Acta Astron., 50, 509

Gray, D. F. 1992, The observation and analysis of stellar photospheres, 2nd edn. (Cambridge University Press)

Maeder, A. & Eenens, P., eds. 2004, IAU Symp. 215: Stellar Rotation

Melo, C. H. F., Pasquini, L., & De Medeiros, J. R. 2001, A&A, 375, 851

Mora, A., Merín, B., Solano, E., et al. 2001, A&A, 378, 116

Reiners, A. 2003, A&A, 408, 707

Reiners, A. & Royer, F. 2004a, A&A, 428, 199

Reiners, A. & Royer, F. 2004b, A&A, 415, 325

Reiners, A. & Schmitt, J. H. M. M. 2003, A&A, 412, 813

Royer, F., Gerbaldi, M., Faraggiana, R., & Gómez, A. E. 2002a, A&A, 381, 105

Royer, F., Grenier, S., Baylac, M.-O., Gómez, A. E., & Zorec, J. 2002b, A&A, 393, 897, (Paper II)

Shajn, G. & Struve, O. 1929, MNRAS, 89, 222

Slettebak, A. 1985, in IAU Symp. 111: Calibration of Fundamental Stellar Quantities, 163

Slettebak, A., Collins, I. G. W., Boyce, P. B., White, N. M., & Parkinson, T. D. 1975, ApJS, 29, 137

Smith, M. A. & Gray, D. F. 1976, PASP, 88, 809

van Belle, G. T., Ciardi, D. R., Thompson, R. R., Akeson, R. L., & Lada, E. A. 2001, ApJ, 559, 1155